Organic Electronics 13 (2012) 579–585

Contents lists available at SciVerse ScienceDirect

Organic Electronics

journal homepage: www.elsevier.com/locate/orgel

Corrugated structure through a spin-coating process for enhanced light extraction from organic light-emitting diodes

Woo Jin Hyun [a], Sang Hyuk Im [b], O Ok Park [a,c,*], Byung Doo Chin [d,*]

[a] Department of Chemical and Biomolecular Engineering (BK21 Graduate Program), Korea Advanced Institute of Science and Technology, 335 Gwahangno, Yuseong-gu, Daejeon 305-701, Republic of Korea
[b] KRICT-EPFL Global Research Laboratory, Advanced Materials Division, Korea Research Institute of Chemical Technology (KRICT), 19 Sinseongno, Yuseong-gu, Daejeon 305-600, Republic of Korea
[c] Department of Energy Systems Engineering, Daegu Gyeongbuk Institute of Science and Technology (DGIST), 50-1, Sang-ri, Hyeongpung-myeon, Dalseong-gun, Daegu 711-873, Republic of Korea
[d] Department of Polymer Science and Engineering, Dankook University, Jukjeon-dong, Suji-gu, Yongin, Gyeonggi 448-701, Republic of Korea

ARTICLE INFO

Article history:
Received 16 November 2011
Received in revised form 3 January 2012
Accepted 3 January 2012
Available online 15 January 2012

Keywords:
Organic light-emitting diodes
Light extraction
Out-coupling structure
Striation
Corrugated structure

ABSTRACT

We have demonstrated a simple fabrication method for an out-coupling structure to enhance light extraction from organic light-emitting diodes (OLEDs). Spin-coating of SiO_2 and TiO_x sol mixture solution develops corrugated film. The structural evolution of the corrugation was explained by the localization of surface tension during the solvent evaporation. The structural parameters of the corrugated structure were characterized by varying the spin-coating speed and the mixing ratio of the solution. Compared to conventional devices, OLEDs with a corrugated structure at the backside of the glass substrate showed increased external quantum efficiency without change in the electroluminescence spectrum. The light extraction enhancement is attributed to the decreased incidence angle at the interface of glass substrate and air.

1. Introduction

Organic light-emitting diodes (OLEDs) have attracted a lot of interest for use in displays and interior lighting due to their promising advantages of low power consumption, high power efficiency, high contrast ratio, and high speed of operation [1,2]. Recently, light extraction from OLEDs has been considered as one of the most important issues for research since less than 20% of the light generated from the emissive layer of a conventionally structured OLED can escape from the device as useful radiation [3,4]. However, most of the generated light is trapped at the interface between the organics/indium tin oxide (ITO) layers ($n_{ITO,organic}$ = 1.7–2) and the glass substrate ($n_{glass} \approx 1.5$) or the glass substrate and air ($n_{air} = 1$) by total internal reflection due to the multiple layered structures with different refractive indices. Therefore, out-coupling of the trapped light is in great demand for high efficiency OLEDs. In order to extract the light confined inside the devices for high external quantum efficiency, defined as the ratio of the number of emitted photons into air to the number of injected electrons, several out-coupling structures have been studied by modifying the shape inside [5–9] and outside the device [10,11]. Some research groups modified the emitting layer to have a light scattering medium inside the film [12] or to have the orientation of the transition dipole moments of organic emitters [13].

Rapid progress has been made in fabrication of out-coupling structures for light extraction from OLEDs; however, those methods require complex and expensive equipment

* Corresponding authors. Address: Department of Chemical and Bio molecular Engineering (BK21 Graduate Program), Korea Advanced Institute of Science and Technology, 335 Gwahangno, Yuseong-gu, Daejeon 305-701, Republic of Korea. Tel.: +82 42 350 3923; fax: +82 350 3910 (O.O. Park), tel.: +82 31 8005 3587; fax: +82 31 8021 7218 (B.D. Chin).
E-mail addresses: ookpark@kaist.ac.kr (O.O. Park), bdchin@dankook.ac.kr (B.D. Chin).

1566-1199/$ - see front matter © 2012 Elsevier B.V. All rights reserved.
doi:10.1016/j.orgel.2012.01.001

with a vacuum system or complicated lithographic process. Considering practical applications, it is essential that fabrication techniques are applicable to a large area and are cost effective, so it is desirable to develop a simple fabrication technique for out-coupling structures. For this purpose, several groups have utilized imprint lithography to fabricate out-coupling structures for enhancing light extraction from OLEDs [14–16]. Although imprint lithography has the advantage of being a vacuum-free process and is easy to fabricate, additional complex steps are still needed to prepare a template for the patterned mold.

In this study, we developed a simple fabrication technique for out-coupling structures without using a mold or vacuum process to enhance the light extraction efficiency of OLEDs. A corrugated structure, as a result of the spatial distribution of the surface tension, can be prepared quickly by a spin-coating process with a small amount of a mixture of SiO_2 and TiO_x sol solution. The width and the height of the corrugation were controlled by the variation of the spin-coating speed and the mixing ratio between two sol solutions. Using standard small molecular emitters, OLEDs with and without the corrugated structure were fabricated, and their device performances were compared. With the introduction of the corrugated structure at the backside glass substrate of the devices, the light trapped from total internal reflection at the interface between the glass substrate and air can be extracted and the out-coupling efficiency is increased.

2. Experimental

2.1. Preparation of SiO_2 and TiO_x sol solutions and their mixture

To prepare the SiO_2 sol solution [17], 0.77 ml of tetraethyl orthosilicate (TEOS), 3.5 ml of (3-glycidoxypropyl) trimethoxysilane (GPTMS), 1.2 ml of methanol, 0.065 ml of acetic acid, and 1 ml of deionized water were mixed by stirring at room temperature for 3 h. Then, 2.6 ml of methanol and 1.9 ml of 2-methoxy ethanol were added to the solution. To prepare the TiO_x sol solution [18], 4.3 ml of titanium tetra isopropoxide (TTIP) was dropped into 5.1 ml of methanol and 0.76 ml of glacial acetic acid was then added to the solution at room temperature. After 30 min, 0.2 ml of deionized water was dropped into the solution and the reaction proceeded for 24 h. At the wavelength of 500 nm, the refractive indices of the SiO_2 layer and TiO_x layer formed with pure sol solutions (annealed at 70 °C) are 1.53 and 1.77, respectively. The SiO_2 and TiO_x sol solutions were mixed with the volume ratios of 35:65, 40:60, and 45:55 and kept in a vortex mixer for 1 h.

2.2. Fabrication of corrugated structure and characterization

The backsides of ITO-coated glass (1 in. × 1 in.) were cleaned and treated with oxygen plasma for 10 min. The mixture solution was dropped (about 100 μl) and spin-coated on the backside of the ITO-coated glass at various spin-coating speeds of 4000, 4500, and 5000 rpm for 30 s. Then, the samples were kept in a convection oven at 70 °C for 10 min. Morphology of the corrugated structure and surface profiles were analyzed with an optical microscope (Nikon, L150) and a Veeco Dektak-8 surface profiler (stylus force, 15 mg; stylus tip radius, 2.5 μm).

2.3. Fabrication of OLEDs and measurement

The ITO surface of substrates with and without the corrugated structure were treated with UV–ozone for 10 min and the following organic layers were deposited by thermal evaporation at a pressure of $<10^{-6}$ Torr: N,N′-di(naphthalene-1-yl)-N,N′-diphenylbenzindine (NPB, 40 nm)/Tris (8-hydroxy quinolinato)aluminum (Alq_3, 50 nm)/lithium fluoride (LiF, 0.5 nm)/aluminum (Al, 100 nm). NPB, Alq_3, LiF, and Al were used as a hole transporting layer, emissive layer, electron injection layer, and a cathode, respectively. The emissive area of the devices is 2×2 mm^2. The current density–voltage–luminance characteristics and the electroluminescence (EL) spectra of the fabricated OLEDs were measured with a Keithley 2400 source measurement unit and a Minolta CS 2000 spectroradiometer.

3. Results and discussion

Fig. 1 contains optical microscope (OM) images of the corrugated structure fabricated by spin-coating a mixture of SiO_2 and TiO_x sol solutions at various spin-coating speeds and several blending ratios. The images show that one-dimensional corrugation is formed along the radial spreading direction of the mixed solution by spin-coating. Fig. 1a–c compare OM images of the corrugated structure fabricated at spin-coating speeds of 5000, 4500, and 4000 rpm and a fixed mixing ratio of 40:60 (SiO_2:TiO_x sol solution, vol./vol.). The OM images were taken at the same radial distance (1 cm) from the center of the glass substrate, where the vertical direction is the radial spreading direction of the mixture solution. Compared to the corrugated structure formed with a spin-coating speed of 5000 rpm, one fabricated with a spin-coating speed of 4500 rpm shows thicker corrugation, and the corrugation formed with a spin-coating speed of 4000 rpm shows even thicker corrugation. These observations indicate that the corrugated structure fabricated with a higher spin-coating speed shows finer corrugation than that formed with a lower spin-coating speed. Fig. 1a, d, and e compare OM images of the corrugated structure fabricated with mixing ratios of 40:60, 45:55, and 35:65 and a fixed spin-coating speed of 5000 rpm. Compared to the corrugated structure fabricated with a mixing ratio of 45:55, the sample formed with a smaller mixing ratio of 40:60 shows thinner corrugation. The corrugated structure formed with a mixing ratio of 35:65 appears almost two-dimensional. The results reveal that finer corrugation can be obtained by using a solution mixture with a smaller mixing ratio of the SiO_2 sol solution as well as spin-coating at a higher spin-coating speed.

The corrugated structure is thickness variation occurred during spin-coating process, which is called striation [19,20]. The thickness variation in spin-coated films has been observed in the sol–gel spin-coating technique

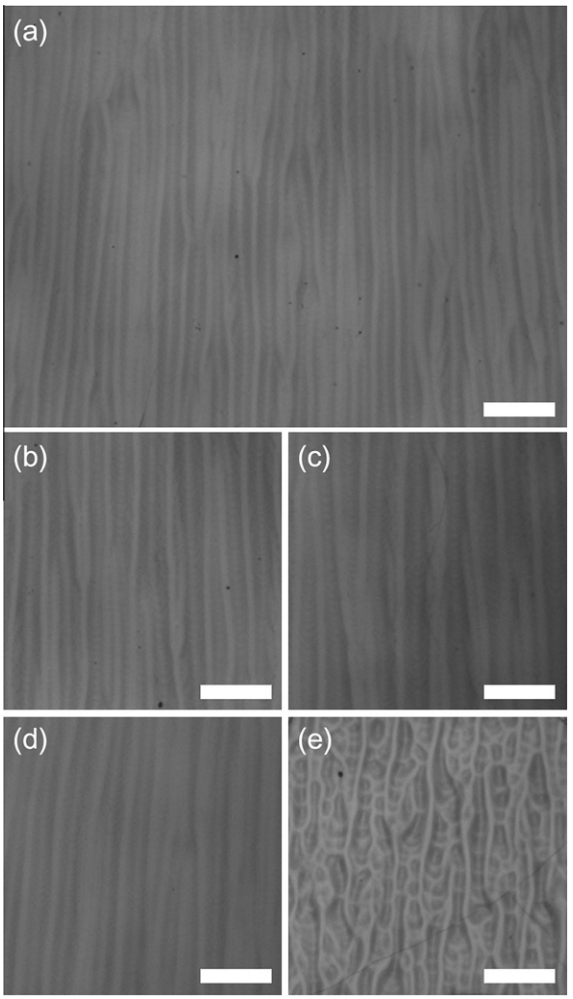

Fig. 1. Optical microscope images of the corrugated structure prepared via a spin-coating process with several spin-coating speeds of (a) 5000, (b) 4500, and (c) 4000 rpm and a fixed mixing ratio of 40:60 (SiO_2:TiO_x sol solution, vol./vol.) and different mixing ratios of (d) 45:55 and (e) 35:65 with a fixed spin-coating speed of 5000 rpm. All scale bars are 300 μm.

[21–23] and spin-coated thin film of single- or multiple-component polymer systems [24–26]. Striation is thought to arisen as a result of the surface tension difference raised during spin-coating process. Fig. 2 illustrates the proposed mechanism of the formation of the corrugated structure via the spin-coating process. Dropped solution is spread and thinned in the early stage of the spin-coating process (Step A). Next, active solvent evaporates (Step B). The evaporation causes the decrease in temperature and the different composition in the local area of the top surface layer, which leads to local variation of surface tension in spin-coated film. Since the area with higher surface tension pulls material from the neighboring area with lower surface tension, which is known as the Marangoni effect [27], the difference in surface tension induces the local fluid motion; the fluids with higher surface tension are confined in the hills while the lower surface tension fluid region forms the valley. The local fluid motion causes the striation of thickness variation in spin-coated film. This

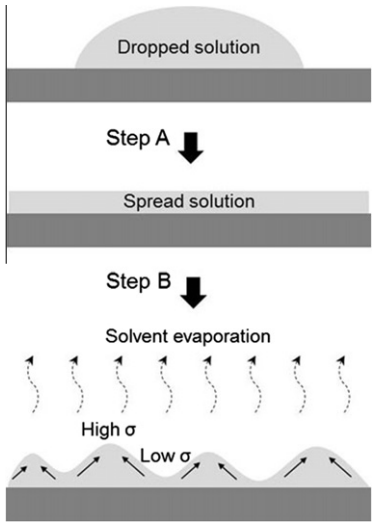

Fig. 2. Schematic diagram of the formation of the corrugated structure developed during the spin-coating process. Diagrams are not to scale.

mechanism for the formation of striation is originally proposed by Haas et al. [20]. At the beginning of this study, we carried out the spin-coating process (5000 rpm, 30 s) with each of the pure solutions: SiO_2 and TiO_x sol. The spin-coated film with pure SiO_2 sol solution shows a flat layer without corrugation. However, the spin-coated film with pure TiO_x sol solution shows the corrugation. We observed that the SiO_2 materials of the coated film is sticky before baking due to the residual solvent of 2-methoxy ethanol (boiling temperature = 125 °C, vapor pressure at 25 °C = 9.5 mmHg), on the other hand, the TiO_x materials of the coated film hardened due to the use of quickly evaporating solvent, right after spin-coating, which indicates the TiO_x materials dry faster than SiO_2 materials. The faster drying rate explains why active solvent evaporation on the coated film during the spin-coating process with TiO_x sol solution increased the formation of the corrugated structure via coating instability: the spin coated TiO_x sol did not have sufficient time to level off owing to the quick drying time, but the flowable spin coated SiO_2 sol did. Although the corrugated structure can be obtained with TiO_x sol solution, due to its poor adhesion to glass substrate and rapid gelation, the coated film peels off the glass substrate a couple minutes after spin-coating. Corrugated film prepared from the SiO_2 and TiO_x sol mixture solution shows good adhesion to the glass substrate (SiO_2 maintains good adhesion as well as slow gelation characteristics). The corrugated film formed with the mixture solution shows good mechanical property. In addition, its structural parameter can be controlled by varying the mixing ratio since the relative difference of the solvent evaporation rate can be changed by precisely controlling the mixing ratio.

In order to analyze the structural parameters of the corrugation, we obtained surface profiles of the structure at the same radial distance from the center of the glass substrate. Fig. 3 shows the surface profiles of the corrugated structure fabricated at spin-coating speeds of 4000 rpm

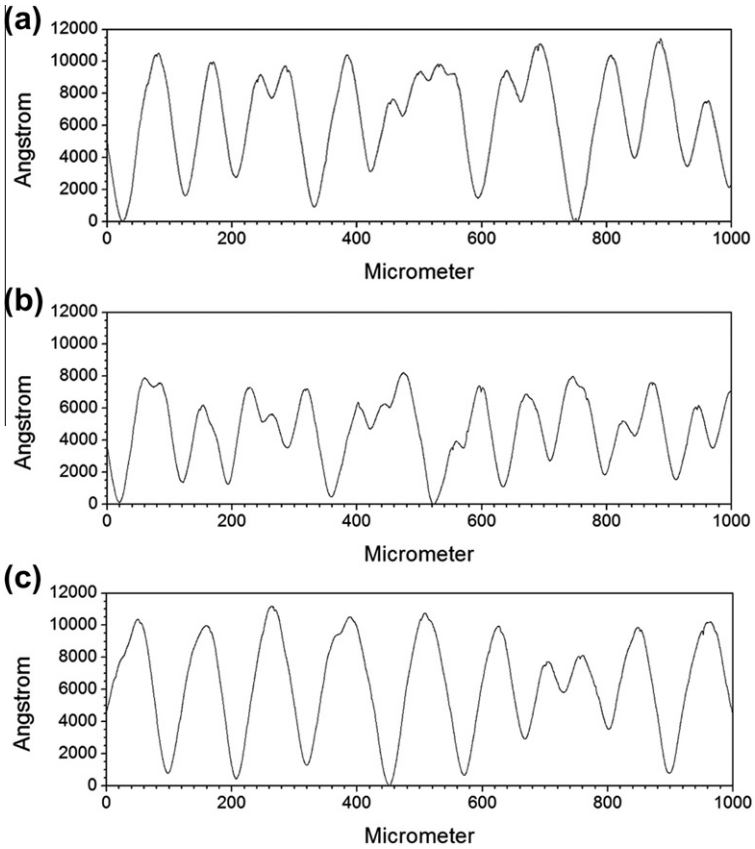

Fig. 3. Surface profiles of the corrugated structure prepared via the spin-coating process with various rotational speeds and mixing ratios of the solution mixture of (a) 4000 rpm and 40:60, (b) 5000 rpm and 40:60, and (c) 5000 rpm and 45:55.

Table 1
Width and height of the corrugated structure prepared via the spin-coating process at various spin-coating speeds of 4000, 4500, and 5000 rpm with a fixed mixing ratio of 40:60 and several mixing ratios of 35:65, 40:60, and 45:55 at a fixed spin-coating speed of 5000 rpm.

Blending ratio (vol./vol.)	Rotational speed (rpm)	Width (μm)	Height (nm)	
40:60	4000	77	974	1D corrugation
40:60	4500	67	828	
40:60	5000	59	675	
45:55	5000	100	987	
35:65	5000	53	765	2D corrugation

(Fig. 3a) and 5000 rpm (Fig. 3b) and a fixed mixing ratio of 40:60. The surface profiles confirm that corrugated structure fabricated at a higher spin-coating speed has more corrugation peaks and its width is smaller. Fig. 3c shows the surface profiles of the corrugated structure fabricated at a spin-coating speed of 5000 rpm with a mixing ratio of 45:55. The surface profile exhibits fewer corrugation peaks and larger width compared to that of the corrugated structure prepared with a higher TiO_x mixing ratio of 40:60 in Fig. 3b. From the surface profiles, we calculated the width and the height of the corrugated structure. The width is calculated from the surface profiles as the total length divided by the number of corrugation peaks; the height is the average of the heights of the peaks. Table 1 shows summaries of the widths and heights of the corrugated structure prepared via the spin-coating process at spin-coating speeds of 4000, 4500, and 5000 rpm with a fixed mixing ratio of 40:60 and with several mixing volume ratios of 35:65, 40:60, and 45:55, at a fixed spin-coating speed of 5000 rpm. The calculated structural parameters of the corrugated structure reveal that the width of the corrugation decreases as the spin-coating speed and the mixing ratio of a TiO_x sol solution increases. Also, the height of the corrugation decreases as the spin-coating speed increases. Both factors lead to faster solvent evaporation, including higher spin-coating speed and mixing ratio of the TiO_x sol solution, promoting a reduction of pattern width by the corrugation, which is similar to the previous study [20].

OLEDs were fabricated with the corrugated structure introduced on the side opposite of the ITO coating as shown in Fig. 4. In order to form the corrugated structure on the entire area (1×1 in.^{2}) of a substrate coupon of the test device, a small amount of mixed solution (about 100 μl) is needed. Prior to device fabrication, samples with the corrugated structure were cleaned once again to remove the possible contamination on the ITO coating

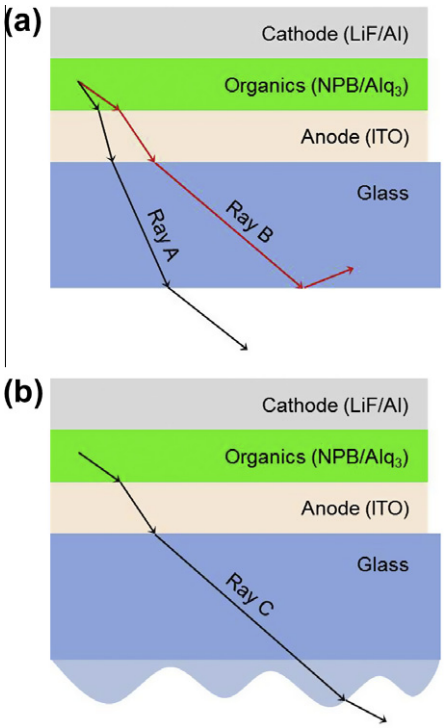

Fig. 4. Schematic diagrams of OLEDs (a) without and (b) with the introduction of the corrugated structure on the backside glass substrate and the mechanisms for light loss and light extraction, respectively, in the devices. Diagrams are not to scale.

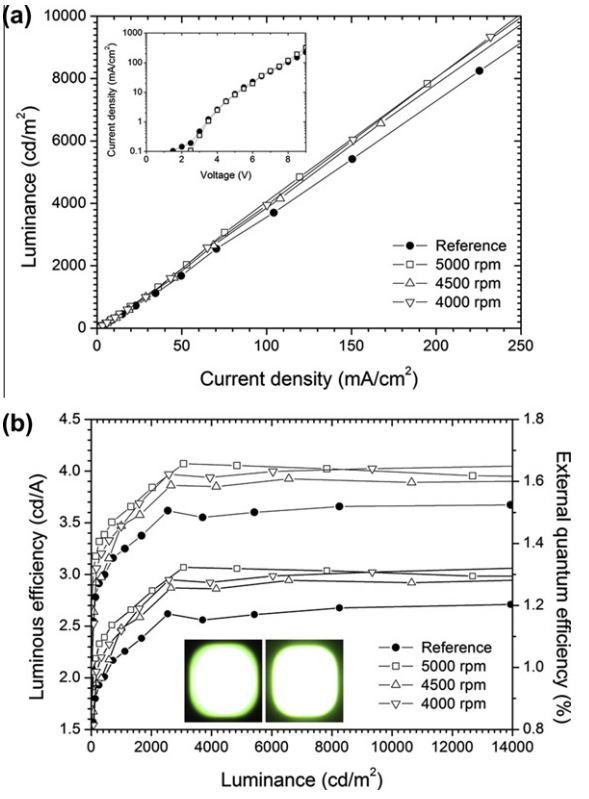

Fig. 5. (a) Luminance versus current density and (b) luminous efficiency–luminance-external quantum efficiency characteristics of the reference OLED and the devices with the corrugated structure fabricated at various spin-coating speeds. Inset of (a): current density versus voltage characteristics of OLEDs with and without the structure. Inset of (b): photographs of OLEDs without (left) and with (right) the structure operating at 30 mA/cm^2.

formed during the previous spin-coating process. The cleaning was carried out using acetone and isopropyl alcohol in an ultrasonic bath. The corrugated structure has good chemical and mechanical properties so that the sonication cleaning does not damage the corrugated structure. We fabricated four devices: one without the corrugated structure for reference and others with the structure prepared at different spin-coating speeds of 4000, 4500, and 5000 rpm at the fixed mixing ratio of 40:60. Fig. 5 displays the performance of the fabricated OLEDs with the corrugated structure prepared at different spin-coating conditions. The devices with the structure show higher luminance than the reference device, as shown in Fig. 5a, which implies that more light generated at the emissive layer was extracted from the device by the introduction of the corrugated structure compared to that without the structure. The current density versus voltage characteristics for the devices with and without the structure show similar behavior, as shown in the inset of Fig. 5a, regardless of the introduction of the out-coupling structure. The enhanced light extraction from the devices can be explained by the decreased incidence angle of light at the interface of the glass substrate and air. In the conventional device shown in Fig. 4a, the light (Ray A) with an incidence angle smaller than the critical angle can pass through the boundary between the glass substrate and air and escape from the device as useful radiation. However, due to the difference in the refractive indices of the air and that of the glass substrate, the light (Ray B) with an incidence angle higher than the critical angle undergoes total internal reflection at the surface of the glass substrate and is confined in the device. On the other hand, the corrugated structure formed at the backside glass substrate reduces the incidence angle of the light (Ray C) as shown in Fig. 4b, so that the total internal reflection can be suppressed and more light can be extracted from the device. As shown in the inset of Fig. 5b, the OLED with the structure shows brighter emission than the device without the structure. Fig. 5b shows the luminous efficiency–luminance-external quantum efficiency characteristics of OLEDs with and without the introduction of the out-coupling structure. Compared to the reference device (typical 3.55 cd/A at 5000 cd/m^2), the device efficiencies with the corrugated structure fabricated at different spin-coating speeds of 4000, 4500, and 5000 rpm and a fixed mixing ratio of 40:60 increased (up to 4.05 cd/A at 5000 cd/m^2).

We also fabricated OLEDs with and without the corrugated structure by varying the mixing ratio of the SiO_2 and TiO_x sol solution. Fig. 6 compares the performance of the devices with and without the structure prepared with mixing ratios of 35:65, 40:60, and 45:55 and a fixed spin-coating speed of 5000 rpm. Luminance versus current density characteristics (Fig. 6a) show that the all devices

with the corrugation show higher luminance at the same current density compared to that of the devices without the structure. As shown in Fig. 6b, using the corrugated structure prepared with the mixed solution of various mixing ratios, the luminous efficiency and the external quantum efficiency of the devices similarly increased, which indicates that the enhancement factor does not show significant dependence on the mixing ratio of the solution mixture as well as the spin-coating speed for the fabrication of the structure.

Fig. 7a presents the normalized EL radiation pattern of the devices with and without the corrugated structure. The radiation profiles of the device with the structure were measured as rotating the device with the axes perpendicular (open triangles) and parallel (open circles) to the one-dimensional corrugation. The measurement of the EL radiation patterns and EL spectra was carried out with an applied current density of 175 mA/cm^2. The radiation pattern with the perpendicular axis is similar to that (filled squares) of a conventional device. On the other hands, the radiation pattern with the parallel axis is slightly changed since the enhanced EL intensity by the corrugated structure depends on the viewing angle. The difference in the radiation pattern with different rotation is attributed to the one-dimensional out-coupling structure affecting the extraction of trapped light mainly waveguided in the direction perpendicular to the striation. Fig. 7b compares EL spectra of the devices with and without the corrugation measured at several viewing angles of 0°, 30°, and 60°. It shows similar EL spectra of the devices with and without the out-coupling structure at the same viewing angle, which implies that the enhanced light emission by the introduction of the corrugated structure does not change the EL spectrum of the device.

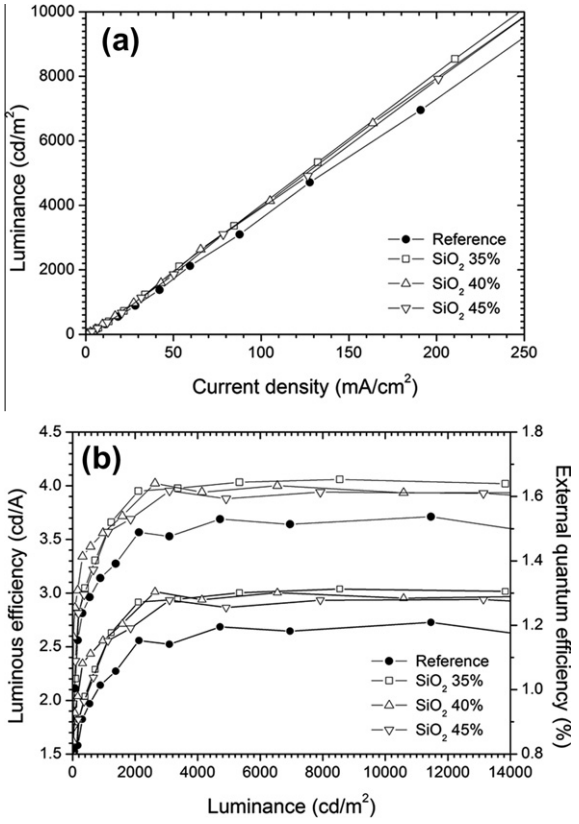

Fig. 6. (a) Luminance versus current density and (b) luminous efficiency–luminance-external quantum efficiency characteristics of the reference OLED and the devices with corrugated fabricated at various mixing ratios of the solution mixture of SiO_2 and TiO_x sol solutions.

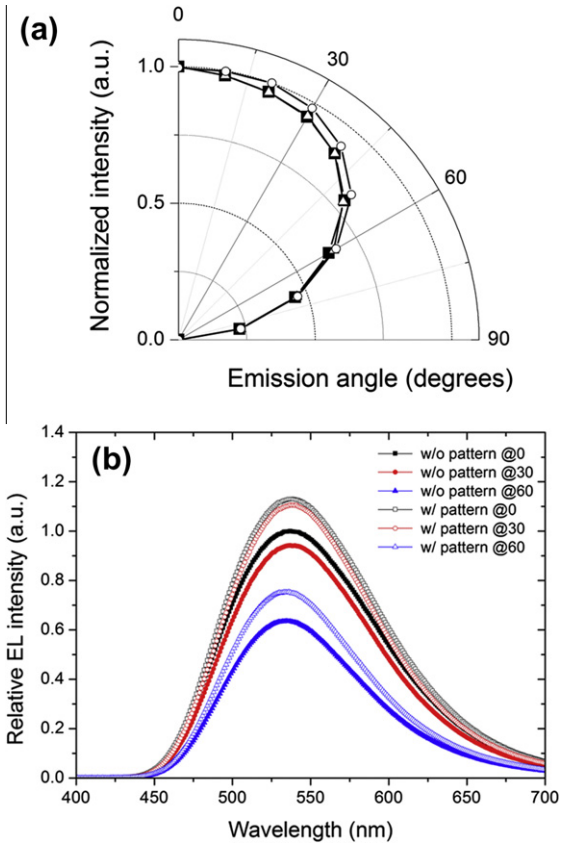

Fig. 7. (a) Normalized EL intensity versus viewing angles and (b) EL spectra at several viewing angles (0°, 30°, and 60°) for OLEDs with and without the corrugated structure. All data were normalized with the intensity of the devices without corrugation in the normal direction.

4. Conclusion

We demonstrate the preparation of the corrugated structure via a spin-coating process for enhancing the light extraction from OLEDs. The one-dimensional corrugated structure is easily obtained by spin-coating with a small amount of mixture of SiO_2 and TiO_x sol solutions. The structural parameters of the corrugation can be controlled by changing the spin-coating speed and the mixing ratio of the solution mixture. The introduction of the structure at the backside glass substrate of OLEDs as an out-coupling structure suppresses the light trapped by total internal reflection at the interface between the glass substrate and air, which leads to the increase of the light extraction efficiency of the device without a change of EL spectrum. We believe that this mold and vacuum-free process could

provide a simple and cost effective way to fabricate out-coupling structures over large area for practical applications.

Acknowledgments

This research was supported by the Basic Science Research Program through the National Research Foundation of Korea (NRF) funded by the Ministry of Education, Science and Technology (CAFDC-20100009894 and 2010-0010039).

References

[1] B.W. D'Andrade, S.R. Forrest, Appl. Phys. Lett. 83 (2003) 3858–3860.
[2] Y. Sun, N.C. Giebink, H. Kanno, B. Ma, M.E. Thompson, S.R. Forrest, Nature 440 (2006) 908–912.
[3] G. Gu, D.Z. Garbuzov, P.E. Burrows, S. Venkatesh, S.R. Forrest, M.E. Thompson, Opt. Lett. 22 (1997) 396–398.
[4] A. Chutinan, K. Ishihara, T. Asano, M. Fujita, S. Noda, Org. Electron. 6 (2005) 3–9.
[5] Y.R. Do, Y.C. Kim, Y.-W. Song, C.-O. Cho, H. Jeon, Y.-J. Lee, S.-H. Kim, Y.-H. Lee, Adv. Mater. 15 (2003) 1214–1218.
[6] Y. Sun, S.R. Forrest, Nat. Photonics 2 (2008) 483–487.
[7] W.H. Koo, S.M. Jeong, F. Araoka, K. Ishikawa, S. Nishimura, T. Toyooka, H. Takezoe, Nat. Photonics 4 (2010) 222–226.
[8] U. Geyer, J. Hauss, B. Riedel, S. Gleiss, U. Lemmer, M. Gerken, J. Appl. Phys. 104 (2008) 093111.
[9] W.J. Hyun, H.K. Lee, S.S. Oh, O. Hess, C.-G. Choi, S.H. Im, O.O. Park, Adv. Mater. 23 (2011) 1846–1850.
[10] S. Möller, S.R. Forrest, J. Appl. Phys. 91 (2002) 3324–3327.
[11] F. Li, X. Li, J. Zhang, B. Yang, Org. Electron. 8 (2007) 635–639.
[12] T.-W. Lee, O.O. Park, Y.C. Kim, Org. Electron. 8 (2007) 317–324.
[13] J. Frischeisen, D. Yokoyama, C. Adachi, W. Brütting, Appl. Phys. Lett. 96 (2010) 073302.
[14] Y. Sun, S.R. Forrest, J. Appl. Phys. 100 (2006) 073106.
[15] K. Ishihara, M. Fujita, I. Matsubara, T. Asano, S. Noda, H. Ohata, A. Hirasawa, H. Nakada, N. Shimoji, Appl. Phys. Lett. 90 (2007) 111114.
[16] S. Jeon, J.-W. Kang, H.-D. Park, J.-J. Kim, J.R. Youn, J. Shim, D.-G. Choi, K.-D. Kim, A.O. Altun, S.-H. Kim, Y.-H. Lee, Appl. Phys. Lett. 92 (2008) 223307.
[17] K.H. Park, S.H. Im, O.O. Park, Nanotechnology 28 (2011) 045602.
[18] D.H. Wang, S.H. Im, H.K. Lee, O.O. Park, J.H. Park, J. Phys. Chem. C 113 (2009) 17268–17273.
[19] D.P. Birnie III, J. Mater. Res. 16 (2001) 1145–1154.
[20] D.E. Haas, D.P. Birnie III, M.J. Zecchino, J.T. Figueroa, J. Mater. Sci. Lett. 20 (2001) 1763–1766.
[21] X.M. Due, X. Orignac, R.M. Almeida, J. Am. Ceram. Soc. 78 (1995) 2254–2256.
[22] H. Kozuka, M. Kajimura, T. Hirano, K. Katayama, J. Sol–Gel Sci. Technol. 19 (2000) 501–504.
[23] S.-B. Jung, T.-J. Ha, H.-H. Park, J. Appl. Phys. 101 (2007) 024109.
[24] F. Zhang, K.G. Jespersen, C. Björström, M. Svensson, M.R. Andersson, V. Sundström, K. Magnusson, E. Moons, A. Yartsev, O. Inganäs, Adv. Funct. Mater. 16 (2006) 667–674.
[25] K.-H. Wu, S.-Y. Lu, H.-L. Chen, Langmuir 22 (2006) 8029–8035.
[26] J.-K. Kim, K. Taki, S. Nagamine, M. Ohshima, Langmuir 24 (2008) 8898–8903.
[27] L.E. Scriven, C.V. Sternling, Nature 187 (1960) 186–188.